EUCLIPSE

EU Cloud Intercomparison, Process Study & Evaluation Project

Grant agreement no. 244067

Deliverable D3.9 Quantification of the cloud-climate feedback and its uncertainty for prescribed large-scale conditions.

Delivery date: 30 months

EUCLIPSE Description of Work: Deliverable 3.9

D3.9: Quantification of the cloud-climate feedback and its uncertainty for prescribed large-scale conditions in the Hadley circulation regime with aid of results of SCMs (current and future climate) and LES (future climate)

Involved EUCLIPSE Partners: MPG, KNMI, METO, CNRS-IPSL, TUD, MF-CNRM,

Aim

Steady-state solutions of cloudy boundary layers at three different locations in the Hadley circulation regime are calculated with LES and fifteen single-column models in order to quantify the change in the net cloud radiative forcing under idealized future climate conditions. July cloud cover is simulated at three different locations over the subtropical Northeast Pacific Ocean which are typified by cold sea surface temperatures (SSTs) under well-mixed stratocumulus ('S12'), cool SSTs under decoupled stratocumulus ('S11'), and shallow cumulus clouds overlying warmer SSTs ('S6'). The idealized climate change includes a uniform 2 K SST increase with corresponding moist-adiabatic warming aloft and subsidence changes, but no change in free-tropospheric relative humidity, surface wind speed, or CO2. For each case, realistic advective forcings and boundary conditions are generated for the control and perturbed states (Zhang et al. 2012b).

1. An introduction to the CGILS experiment

Bony and Dufresne (2005) found much of the variability in the cloud-climate feedback in global climate models to be due to differences in the climate change response of marine boundary layer cloud in low-latitude ocean regions under mean subsidence. CFMIP (the Cloud Feedback Model Intercomparison Project) and GASS (GEWEX (Global Energy and Water Cycle Experiment) Atmospheric System Study) initiated a joint project -- CGILS (the CFMIP-GASS Intercomparison of Large Eddy Models (LESs) and Single Column Models (SCMs)) to analyze the physical mechanisms of low cloud feedbacks by using a simplified experimental setup. The objective of CGILS is

- to investigate how low clouds respond to a hypothetical climate warming in atmospheric models and the associated physical mechanisms.

The initial focus of CGILS is on low clouds in the subtropics, because several studies have demonstrated that these clouds contribute significantly to model differences of cloud feedbacks. The role played by these clouds is consistent with the fact that low clouds have the largest net cloud radiative effect, in contrast to deep clouds in which the positive longwave and negative shortwave cloud effects largely cancel out. Figure 1 shows the distribution of low clouds in the northern summer (June to August) from a composite of the A-train integrated CALIPSO, CloudSat, CERES, and MODIS merged satellite product (C3M) averaged from 2006 to 2009.

The objective of CGILS is to investigate how these low clouds respond to a hypothetical climate warming in atmospheric models and the associated physical mechanisms. The CGILS experimental setup is similar to Zhang and Bretherton (2008), but with modifications. Summertime-mean boundary conditions and advective forcing are specified at three locations along the GCSS/WGNE Pacific Cross Section Intercomparison (GPCI) in the northeastern

subtropical Pacific (Teixeira et al. 2011), at which the three primary cloud regimes are shallow cumulus, cumulus under stratocumulus, and well-mixed stratocumulus. For simplicity of description, these three cloud types are referred to as shallow cumulus, stratocumulus, and coastal stratus respectively in this paper. Some key details of the large-scale conditions are presented in Figure 2. As a surrogate of a warmer climate, the sea-surface temperature (SST) is uniformly raised by 2 degrees as in Cess et al. (1990); the free troposphere is assumed to respond moist-adiabatically, and the amplitude of the large-scale subsidence is then inferred from a column energy balance. Clouds are simulated in the control and the warmer climates by using SCMs and LESs steadily forced by the control and perturbed conditions. The differences of clouds between the warmer and control climates are then investigated.

The participating LES and single-column models and their acronyms are summarized in Tables 2 and 3. Some modeling groups submitted results from more than one version of their SCM. If the SCM had a parent GCM that is participating in CMIP5, we only include the SCM version that used that GCM's default physical parameterization package. For LES models, we used all submitted results. The resolution in the boundary layer (PBL) is typically not sufficient to resolve observed thin clouds in the SCMs. No attempt is made to make them finer since our objective is to understand the behavior of the operational GCMs. For the LES models, however, because they are intended as benchmarks, much higher vertical resolution is used.

2. SCM and LES results

2.1. Control case

The differences among all models can be seen in the time-averaged cloud profiles in Figure 3, from S6 in the top row to S12 in the bottom row. SCMs results are in the left column; LES models in the middle column; observations from C3M in the right column for the summers of 2006 to 2009. Note that the observations may have categorized drizzles as clouds, therefore having a different definition of clouds from that in the models. The blue lines denote the ensemble averages or multi-year averages; the red lines denote the 25 and 75 percentiles.

Despite large differences among the models, the intended shallow cumulus, stratocumulus, and coastal stratus are generally simulated. The values of the ensemble average of the SCMs and the LES models, and the cloud-top altitudes lie close to the range of the observations, even though the models used constant large-scale forcing. The spread in the LES models is much smaller than that in the SCMs, but they tend to overestimate the cloud peak height at S11 and S12 relative to observations. This is at least partially due to the idealized setup in which the large scale subsidence does not respond to clouds and the forcing is constant. The use of the same forcing for all models may have exaggerated the inter-model differences in the SCMs, especially in the depth of the capping inversion, since in GCMs the large scale circulation can respond to local differences in the inversion height to partially compensate them (Blossey et al. 2009).

2.2. Perturbed climate

For the given climate perturbation, the SCMs differ greatly in their cloud feedbacks with both positive and negative signs for all three regimes (see Figure 4). In the SCMs, the two dominant cloud feedback processes are found to be caused by enhanced surface-driven boundary turbulence and shallow convection in a surrogate climate warming: The former leads to a negative cloud feedback; the latter causes a positive feedback. Below we will

explain in more detail the results for each selected low cloud regime.

2.2a. Stratocumulus (S11)

Figure 4b shows the change of net cloud radiative forcing (CRF) from the control to the warmer climate at S11 in all models. Increase of CRF means positive cloud feedbacks; decrease of CRF means negative feedbacks. Among the 15 SCMs, seven showed positive feedback; seven showed negative feedbacks; one showed very little feedback. Among the four LES models that completed the simulations, two showed positive feedback, two showed little feedback. The models also differ greatly in the magnitude of the feedbacks. Because of the simplified setup in CGILS, we will only focus on the signs of the feedbacks in this study.

The first robust feature of all models is the increase of surface latent heat flux (LHF) in a warmer climate. This is shown in Figure 5. It can be explained intuitively as follows: the atmospheric column has two moisture boundary conditions. At the lower boundary, its value increases with SST, but at the upper boundary, it is fixed with a small value because the region is under large-scale subsidence. A larger contrast between the lower and top boundaries should lead to a larger flux from the surface to the atmosphere.

The increased LHF needs to be balanced by an equivalent amount of drying to the PBL in a warmer climate. This drying can be accomplished either by an increase in the net condensation and a subsequent increase in the precipitation, or by enhanced mixing with the free tropospheric air. In the SCMs an increase in the cloud liquid water will yield a negative cloud feedback; in LES models this may be different because the relationship between condensation and cloud water is more complex when averaged over the simulation domain. If the drying is through enhanced mixing with free tropospheric air, the cloud layer may be diluted, which tends to create a positive cloud feedback. In some models, both mechanisms can operate.

2.2b. Shallow cumulus (S6) and coastal stratus (S12)

Cloud feedbacks from all models at the shallow cumulus location (S6) are shown in Figure 4a. Five SCMs simulated positive cloud feedback; ten simulated negative feedback. None of the LES models simulated negative feedback; most of them simulated a modest positive cloud feedback. This modest amount is related with the small cloud amount simulated by the LES, but it can be important because shallow cumulus covers large areas in the subtropics.

The large-scale environment at S6 has higher SST and weaker subsidence than at S11, affecting the SCM parameterized processes in several ways: *(1)* The PBL is higher at S6 than S11, and the shallow convection can reach well above the PBL top. Even though convection can still dilute clouds in the PBL, it can also create its own clouds at its detrainment level because the moisture difference between the cloudy and clear air is much smaller at S6 than at S11. *(2)* Depending on how convective entrainment and clouds are parameterized, convective mass flux can either increase or decrease in a warmer climate in a particular model, which is different with the case at S11 where convection is restricted to a thinner layer. *(3)* Because of the higher altitude, the change in longwave CRF also contributes to the differences in modeled cloud feedbacks.

Despite these differences, the feedback signs in ten of the 15 SCMs are the same at S11 and S6. Indeed, similar dominant mechanisms are operating in the SCMs at the two locations, i.e., the creation of low clouds by the PBL scheme, and the dilution of them by the shallow convection. But on top of the dilution effect, shallow convection can additionally create clouds at the detrainment levels. Depending on how the shallow convection is parameterized, the SCM cloud feedback can change sign between S6 and S11. For the LESs, the dependence

of precipitation on the depth of the shallow cumulus layer is a critical control on the boundary layer depth and its response to forcing perturbations; for the SCMs however, the vertical resolutions are too coarse to describe this process. The fact that the LES models agree but the SCMs differ point to the need for improving the shallow convection parameterization schemes in the SCMs.

Figure 4c shows the cloud feedback at S12, where the SST is colder and subsidence is stronger than those at S11. Six SCMs simulated positive cloud feedback; seven simulated negative feedback; two simulated little feedback. Out of the six LES models, five of them simulated a negative feedback, with the only exception of DALES that simulated a positive cloud feedback. While results from the LES models are not conclusive, they point to a cautionary consensus.

3. LES sensitivity tests

3.1. Separation of the thermodynamic component of cloud feedback in S12

The default CGILS climate change consists of a thermodynamic warming and a subsidence reduction, resulting in the perturbed case P2S. For case S12, all LES models also ran case P2, which included the thermodynamic warming but not the subsidence reduction; this is roughly analogous to the partitioning of tropics-wide cloud feedbacks into thermodynamic and dynamic components proposed by Bony et al. (2004). Cloud changes from the CTL to P2 simulations represent a sensitivity to thermodynamic changes, while cloud changes between the P2 and P2S simulations reflect a sensitivity to dynamic (subsidence) changes.

Figure 6 shows time-height cross-sections of cloud fraction from the CTL, P2 and P2S simulations from DALES; these are broadly representative of the evolution of all the models. The inversion rises slightly to comparable steady-state heights in CTL and P2, but the cloud layer becomes slightly thinner in P2. The inversion deepens more and the cloud layer thickens in the P2S simulation. The sharp transition in cloud fraction across the mean cloud base in CTL and P2 is indicative of a well-mixed boundary layer in which all updrafts have a similar lifting condensation level (LCL); in P2S this transition is less sharp, suggesting incipient decoupling.

When the subsidence is reduced in the P2S simulations, the equilibrium cloud top and cloud base heights rise by more than 100 m from their values in the P2 simulations. In all models, the separation distance between stratocumulus cloud base and the LCL increases, suggesting that the deeper boundary layers in the P2S simulations are marginally decoupled. The LWP increases from P2 to P2S by 30-50%, and SWCRE strengthens by 18-37 W m^{-2}, consistent with observational findings (manuscript to be submitted by Myers and Norris, 2012). The contrasting responses of the cloud to thermodynamic and dynamic changes are depicted in figure 7, where the changes in shortwave cloud radiative effect (SWCRE) from CTL to P2 and from P2 to P2S are shown as a function of inversion height for each model. While the CTL simulations differ in their equilibrium LWP and inversion height, the their responses to thermodynamic and dynamic changes are qualitatively similar.

4. Conclusions and outlook

Zhang et al. (2012a) summarize the main findings of the SCMs as follows:

- Simulated low clouds in the SCMs are largely the results of moistening from the PBL turbulence schemes, reinforced by the radiative cooling at the cloud tops; they are diluted

by the shallow convection and cloud top entrainment schemes. These schemes differ greatly among the models, leading to very different cloud fields.

- In the surrogate climate change of warmer SST, two robust changes of the SCMs in the stratocumulus regimes are the increase of surface latent heat flux and the increase of convective mass flux. The first acts to produce a negative cloud feedback, similar to a well-mixed layer model; the second acts to cause a positive feedback. These mechanisms may operate together in a model. The net effect depends on specifics such as local versus nonlocal diffusivity, launching level and mass flux profile of shallow convection. Key elements are the roles of increases of PBL turbulence and shallow convection mass flux in a warmer climate.

- For shallow cumulus, the convective mass fluxes in SCMs can either increase or decrease in a warmer climate; they can also either dilute the boundary layer to dissipate clouds or to create clouds at the detainment level. These effects add to the effect of the PBL turbulence on cloud feedback.

The LES results for CGILS are reported in detail by Blossey et al. (2012). For the control climate, the LESs correctly produce the expected cloud type at all three locations. With the perturbed forcings, all models simulate boundary-layer deepening due to reduced subsidence in the warmer climate, with less deepening at the warm-SST location due to regulation by precipitation. The models do not show a consistent response of liquid water path and albedo in the perturbed climate, though the majority predict cloud thickening (negative cloud feedback) at the cold-SST location and slight cloud thinning (positive cloud feedback) at the cool-SST and warm-SST locations, respectively. In perturbed climate simulations at the cold-SST location without the subsidence decrease, cloud albedo consistently decreases across the models. Thus, boundary-layer cloud feedback on climate change involves compensating thermodynamic and dynamic effects of warming, and may interact with patterns of subsidence change.

So in conclusion the LES results do provide guidance on the cloud feedbacks and suggest, given the applied CGILS set up and perturbations:

- Well-mixed Stratocumulus (S12) is mostly characterized by a negative cloud feedback
- Stratocumulus with underlying cumulus (S11) is characterized by a positive cloud feedback
- Trade Wind Cumulus (S6) is characterized by a (small) positive feedback

The open question is to what extend these results can be generalized for a wider range of large scale conditions under which these cloud types are subjected in the real world and in climate models. We therefore will continue the CGILS experiments in a broadened phase space as proposed by De Roode et al. (2012). They discuss stratocumulus equilibrium states as calculated with a mixed-layer model as a function of the lower tropospheric stability and the specific humidity in the free troposphere. In contrast to CGILS, in order to quantify the LWP response they perturb only one single cloud controlling factor like, for example, the large-scale divergence, sea surface temperature, horizontal wind velocity. One of the major benefits of the phase space is that it helps to identify where models locate the regime change from stratocumulus to shallow cumulus. Furthermore, the perturbation of a single external factor can give some clear insight in the general behaviour of the parameterization scheme. For example, it would be interesting to quantify the moistening of the boundary layer and the

change in the cloud-top height in SCM simulations in which only the sea surface temperature is perturbed. Such an approach is also applicable to SCMs, as will be demonstrated by Dal Gesso et al. (to be submitted, 2013).

Bibliography

Blossey, P. N., C. S. Bretherton, and M. C. Wyant, 2009: Understanding subtropical low cloud 552 response to a warmer climate in a superparameterized climate model. Part II: Column 553 modeling with a cloud-resolving model. *Journal of Advancing Modeling Earth Systems*, 1, 14 pp., doi:10.3894/JAMES.2009.1.8 .

Cess, R. D, and Coauthors, 1990: Intercomparison and interpretation of cloud-climate feedback processes in nineteen atmospheric general circulation models. *J. Geophys. Res.*, **95**, 16 601–16 615.

Teixeira, J., and Coauthors, 2011: Tropical and Subtropical Cloud Transitions in Weather and Climate Prediction Models: The GCSS/WGNE Pacific Cross-Section Intercomparison (GPCI). *J. Climate*, **24**, 5223–5256.

Zhang, M., and C. S. Bretherton, 2008: Mechanisms of low cloud climate feedback in idealized single-column simulations with the Community Atmospheric Model (CAM3). *J. Climate*, **21**, 4859-4878.

4. EUCLIPSE relevant documents and papers

4.2 Papers

The papers below are made available for downloading from the world-wide-web.

Blossey, P. N., C. S. Bretherton, M. Zhang, A. Cheng, S. Endo, T. Heus, Y. Liu, A. Lock, S. R. de Roode and K.-M. Xu, 2012: Marine low cloud sensitivity to an idealized climate change: The CGILS LES Intercomparison. Accepted pending minor revisions, *J. Adv. Model. Earth Syst.*
http://www.euclipse.eu/Publications_new.html

Bony, S., J.-L. Dufresne, H. L. Treut, J.-J. Morcrette, and C. Senior (2004), On dynamic and thermodynamic components of cloud changes, *Clim. Dyn.*, **22** (2-3), 71–86, doi:10.1007/s00382-003-0369-6.
http://www.euclipse.eu/Publications_new.html

Zhang, M. and 39 co-authors, 2012a: CGILS: First Results from an International Project to Understand the Physical Mechanisms of Low Cloud Feedbacks in General Circulation Models. Submitted to the *Bull. Amer. Met. Soc.*
http://www.euclipse.eu/Publications_new.html

Zhang, M., C. S. Bretherton, P. N. Blossey, Sandrine Bony, F. Brient and J.-C. Golaz, 2012b:

The CGILS experimental design to investigate low cloud feedbacks in general circulation models by using single-column and large-eddy simulation models. Submitted to the *J. Adv. Model. Earth*.
http://www.euclipse.eu/Publications_new.html

de Roode, S.R., A. P. Siebesma, S. Dal Gesso, H. J. J. Jonker, J. Schalkwijk, and J. Sival, 2012: The stratocumulus response to a single perturbation in cloud controlling factors. Submitted to the J. Clim.
http://www.euclipse.eu/Publications_new.html

Tables

	S6 shallow cumulus	S11 stratocumulus	S12 stratus
Latitude (Degrees North)	**17^{o}N**	**32^{o}N**	**35^{o}N**
Longitude (Degrees)	**149^{o}W**	**129^{o}W**	**125^{o}W**
SLP (mb)	**1014.1**	**1020.8**	**1018.6**
SST (^{o}C)	**25.6**	**19.3**	**17.8**
Tair_surface (^{o}C)	**24.1**	**17.8**	**16.3**
U_surface (m/s)	**-7.4**	**-1.8**	**2.1**
V_surface (m/s)	**-2.7**	**-6.5**	**-8.0**
RH_surface (m/s)	**80%**	**80%**	**80%**
Mean TOA insolation (W/m^{2})	**448.1**	**471.5**	**473.1**
Mean daytime solar zenith angle	**51.0**	**52.0**	**52.7**
Daytime fraction on July 15	**0.539**	**0.580**	**0.590**
Eccentricity on July 15	**0.967**	**0.967**	**0.967**
Surface Albedo	**0.07**	**0.07**	**0.07**

Table 1: Location and surface meteorological conditions at the three locations.

Models Acronyms	Model Institution	References	Participants
ACCESS (Australian Community Climate and Earth System Simulator)	Australian Commonwealth Scientific and Industrial Research Organisation/Centre for Australian Weather and Climate Research	Hewitt et al. (2011)	Charmaine Franklin
CAM4 (Community Atmospheric Model Version 4)	National Center for Atmospheric Research (NCAR), USA	Neale et al. (2012a)	Minghua Zhang, Cecile Hannay, Philip Rasch
CAM5 (Community Atmospheric Model Version 4)	National Center for Atmospheric Research (NCAR), USA	Rasch et al. (2012), Neale et al. (2012b)	Minghua Zhang, Cecile Hannay, Philip Rasch
CCC (Canadian Centre for Climate)	Canadian Centre for Climate Modelling and Analysis, Canada	Ma et al. (2010)	Phillip Austin, Knut von Salzen
CLUBB (Cloud Layers Unified By Binormals)	University of Wisconsin at Milwaukee, USA	Golaz et al. (2002a,b), Larson and Golaz (2005), Golaz et al. (2007)	Vincent Larson, Ryan Senkbeil
ECHAM6 (ECMWF-University of Hamburg Model Version 6)	Max-Planck Institute of Meteorology, Germany	Roeckner et al. (2011), Stevens et al.(2012)	Suvarchal Cheedela, Bjorn Stevens
ECMWF (European Center for Medium Range Weather Forecasting)	European Center for Medium Range Weather Forecasting	Neggers et al (2009a, 2009b)	Martin Koehler
EC-ETH (ECMWF- Eidgenössische Technische Hochschule)	Swiss Federal Institute of Technology, Switzerland	Isotta et al. (2011)	Colombe Siegenthaler-Le Drian, Isotta Alessandro Francesco ,Ulrike Lohman
GFDL-AM3 (Geophysical Fluid Dynamics Laboratory Atmospheric Model Version 3)	NOAA Geophysical Fluid Dynamics Laboratory, USA	Donner et al. (2011)	Jean-Christophe Golaz, Ming Zhao
GISS (Goddard Institute for Space Studies)	NASA Goddard Institute for Space Studies, USA	Schmidt et al. (2006)	Anthony DelGenio, Audrey Wolf
GMAO (NASA Global Modeling and Assimilation Office)	NASA Goddard Space Flight Center, USA	Bacmeister et al. (2006)	Andrea Molod, Max Suarez, Julio Bacmeister
HadGEM2 (Hadley Centre Global Environment Model version 2)	Met Office, United Kingdom	Lock et al. (2001), Martin et al. (2011)	Adrian Lock, Mark Webb
JMA (Japanese Meteorological Agency)	Japanese Meteorological Agency, Japan	Kawai (2012)	Hideaki Kawai
IPSL (Institute Pierre Simon Laplace)	Institute Pierre Simon Laplace (IPSL), France	Bony and Emanuel (2001), Hourdin et al. (2006)	Florent Brient, Sandrine Bony, Jean-Louis Dufresne
RACMO (Regional Atmospheric Climate Model**)**	Royal Netherlands Meteorological Institute, the Netherlands	Neggers et al (2009a, 2009b)	Roel Neggers, Pier Siebesma

Table 2: List of SCM participants

DALES (Dutch Atmospheric. Large-Eddy Simulation)	Royal Netherlands Meteorological Institute, the Netherlands	Heus et al. (2010)	Stephan de Roode
SAMA (System for Atmospheric Models)	University of Washington/Stony Brook University, USA	Khairtoutdinov and Randall (2003), Bretherton et al. (2012)	Peter Blossey, Chris Bretherton, Marat Khairoutdinov
UCLA (University of California at Los Angeles)	Max Plank Institute of Meteorology, Germany/University of California at Los Angeles, USA	Stevens et al. (2005), Stevens and Seifert (2008)	Thijs Heus, Irina Sandu, Bjorn Stevens
LARC (NASA Langley Research Center)	NASA Langley Research Center, USA	Xu et al. (2010)	Anning Cheng, Kuan-man Xu
MOLEM2 (Met Office Large Eddy Model)	Met Office, United Kingdom	Lock (2009)	Adrian Lock
WRF (Weather Research and Forecasting)	National Center for Atmospheric Research/Brookhaven National Laboratory	Endo and Liu (2012)	Satosh End, Yangang Liu

Table 3: List of LES participants

Figures

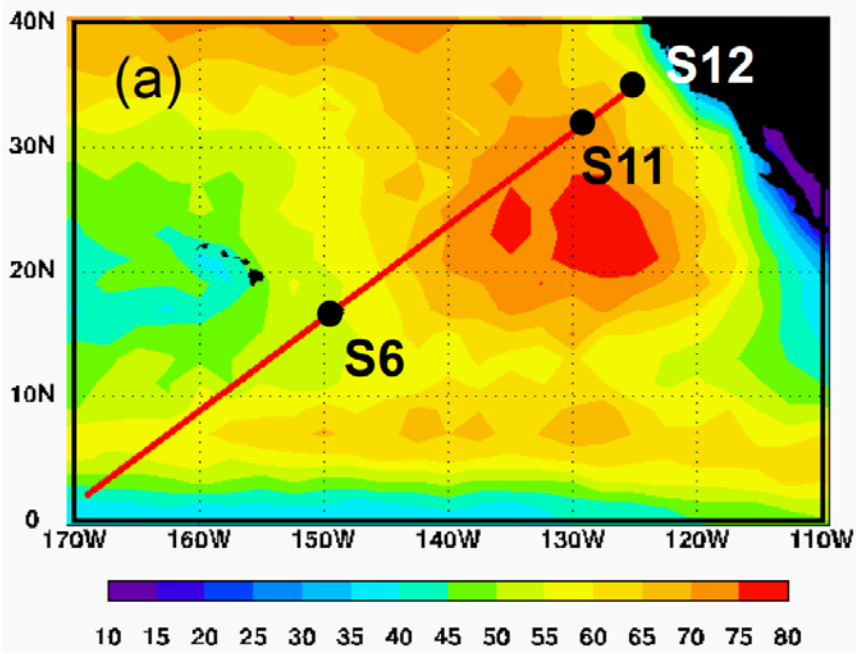

Figure 1. Averaged amount of low clouds in June-July-August (%). The red line is the northern portion of the GPCI. The symbols 'S6', 'S11' and 'S12' are the three locations used in the CGILS experiments (From Zhang et al., 2012a).

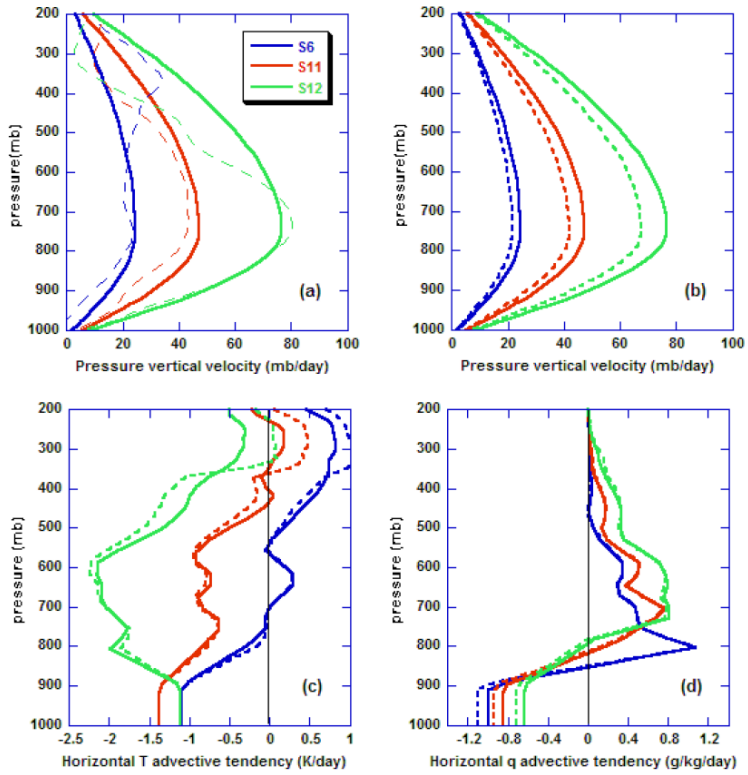

Figure 2: (a) Large-scale pressure vertical velocity (subsidence) at the three locations in the control climate (solid lines), and in the ERA-Interim (dashed lines). (b) Same as (a) except that the dashed lines denote subsidence rates in the warmer climate. (c) Same as (b) except for horizontal advective tendency of temperature. (d) Same as (b) except for horizontal advective tendency of water vapor.

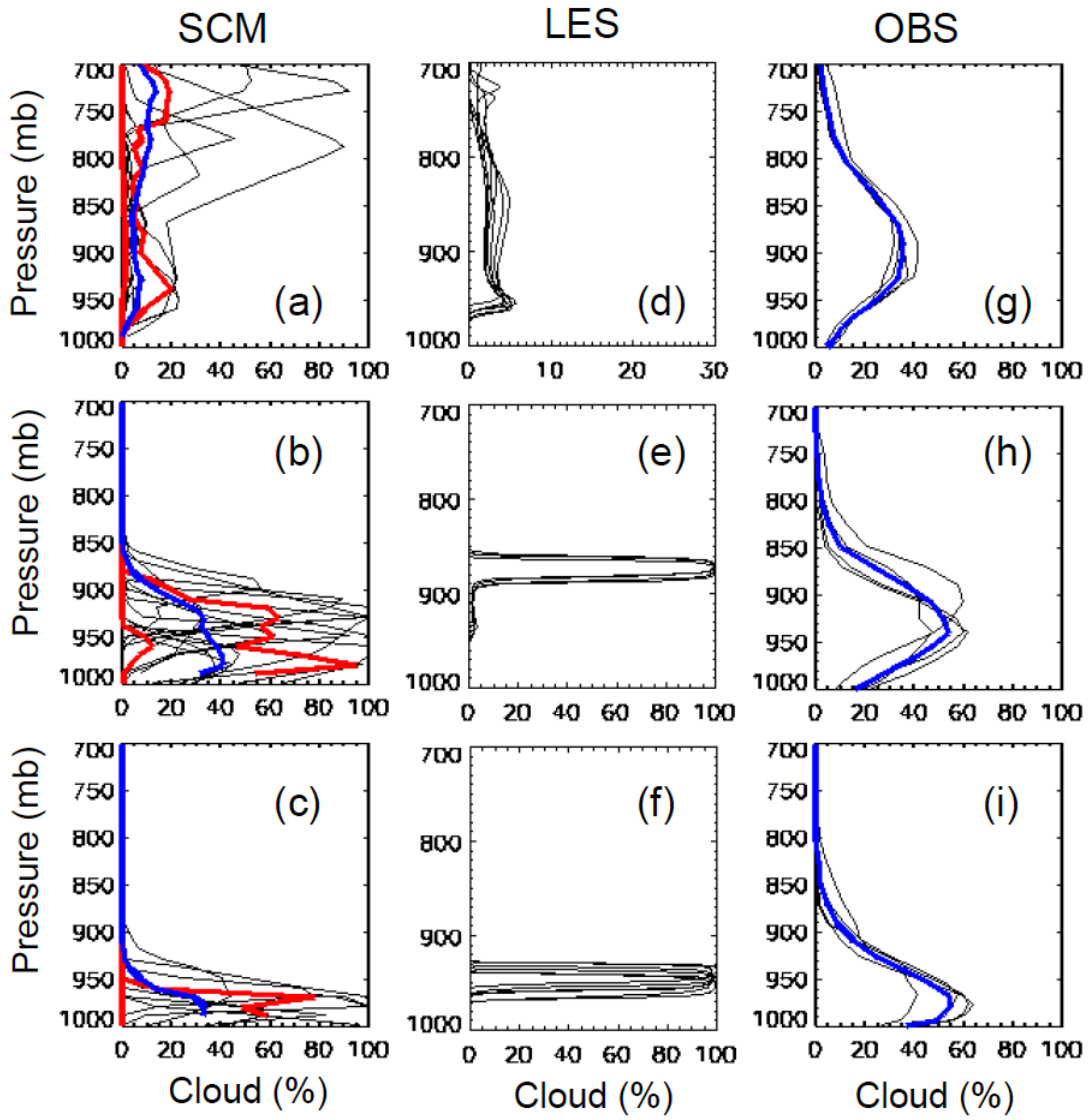

Figure 3: (a)-(c) are the averaged profiles of cloud amount (%) by SCMs for S6, S11 and S12 respectively (from top to bottom panels). (d)-(f) are the same as (a)-(c) but by the LES models. (g)-(i) are from the C3M satellite measurements. The blue lines are ensemble averages; the red lines are the 25% and 75% percentiles.

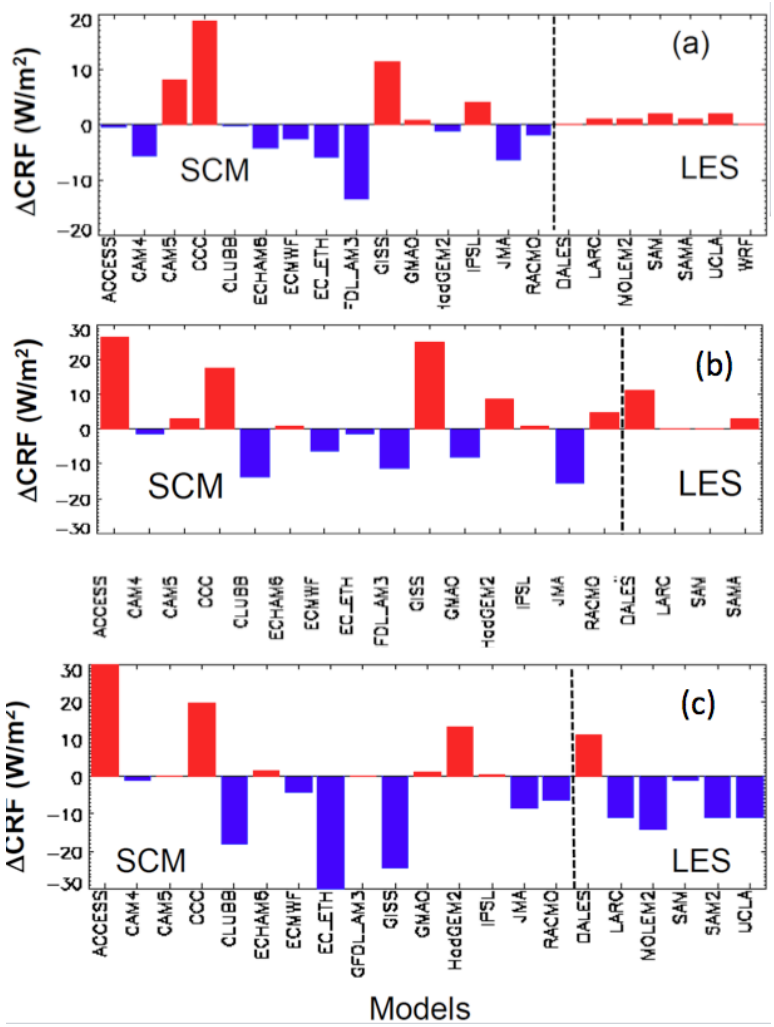

Figure 4. Cloud feedback ΔCRF at S6 (a), S11 (b), and S12 (c), from Zhang et al. (2012a).

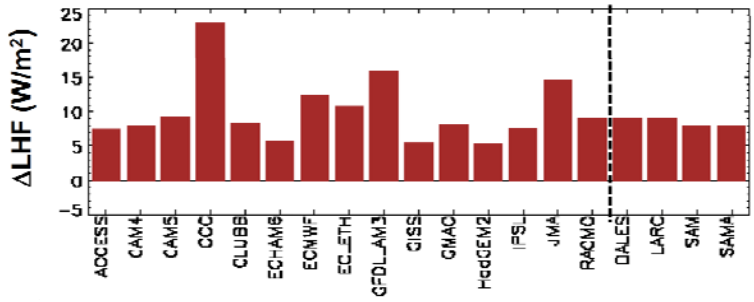

Figure 5. Change in the latent heat flux ΔLHF at S11 , from Zhang et al. (2012a).

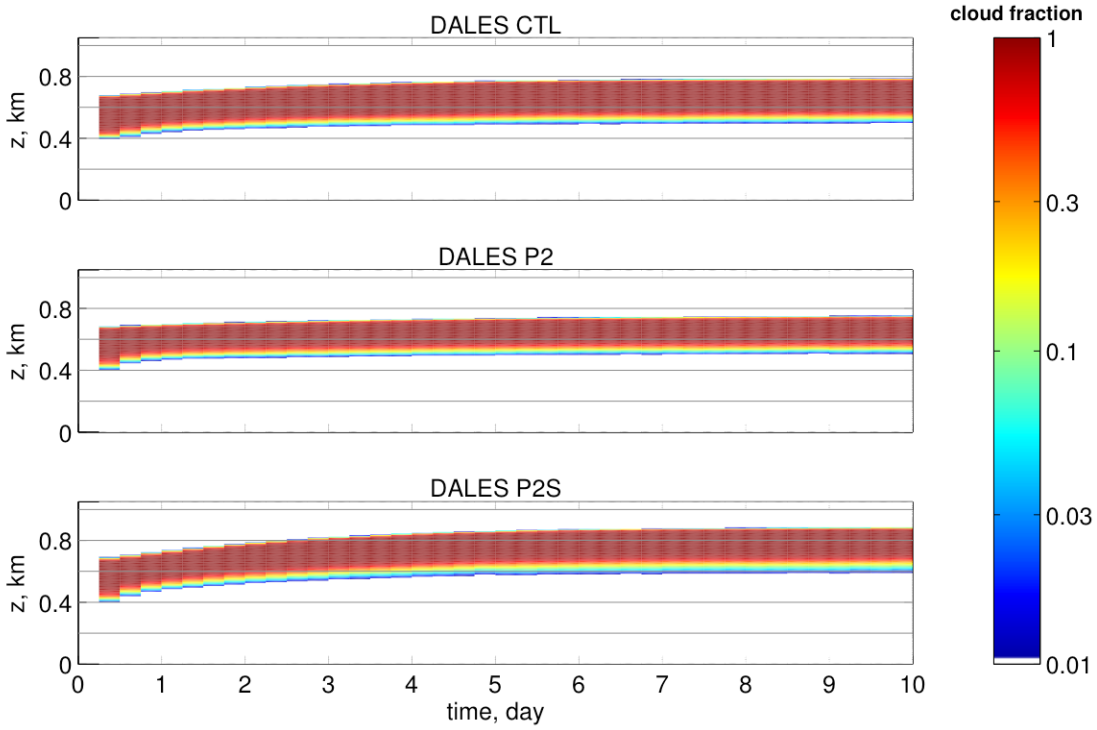

Figure 6. Time-height profiles of cloud fraction for the S12 control, P2 and P2S simulations from DALES.

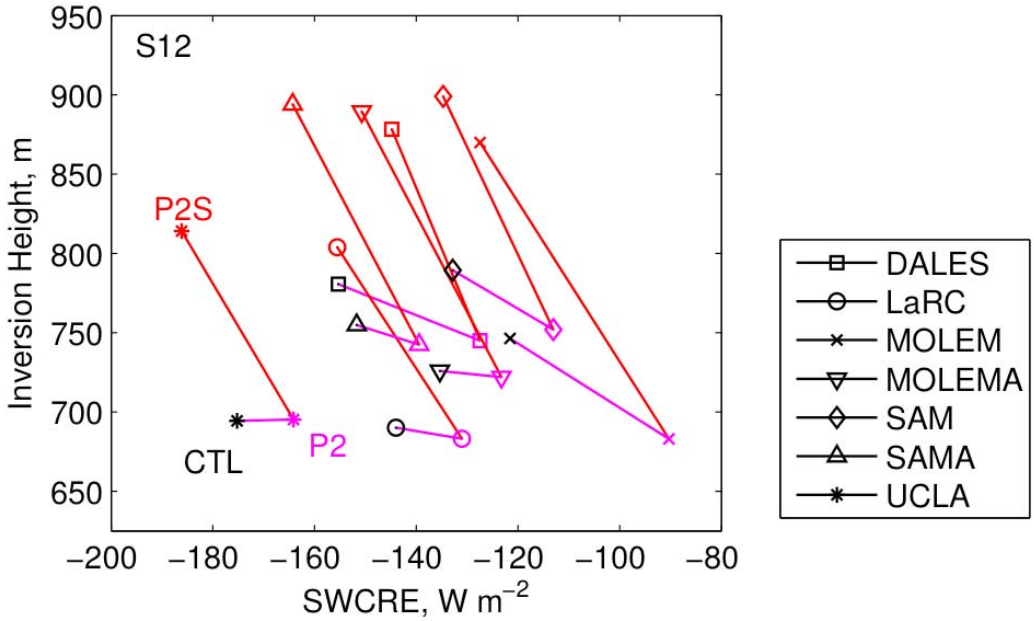

Figure 7. Scatter plot of inversion height and shortwave cloud radiative effect from the CTL, P2 and P2S simulations for each of the CGILS models at S12. Lines connect the CTL, P2 and P2S simulations from each model.